Journal of Oil Palm Research Vol. 37 (4) December 2025 p. 719-728
DOI: https://doi.org/10.21894/jopr.2024.0056

INSIGHT INTO FATTY ACID-AMINO ACIDS INTERACTIONS IN LIPASE ENZYME CATALYSIS OF TRANSESTERIFICATION REACTION OF PALM OIL USING DENSITY FUNCTIONAL THEORY B3LYP 6-31G(D,P)

RADIAH ALI[1]; ALYZA AZZURA AZMI[1] and SABIQAH TUAN ANUAR[1]*

ABSTRACT

This study elucidates the effects of various triacylglycerol (TAG) fatty acid constituents consist of palmitoyl, oleoyl and linoleoyl on the enzymatic transesterification of palm olein and discusses the synergistic effect between substrates and lipase (amino acid). Quantum mechanical calculations of Gaussian09 and density functional theory (DFT) at the B3LYP 6-31G(d,p) level were employed to evaluate their physical parameters including total electronic energy, high-occupied molecular orbital (HOMO), lowest-unoccupied molecular orbital (LUMO), energy band gap, hardness, softness, global electronegativity, dipole moment and interaction energy. The results showed that the interaction energy is the main contributor to the performance of the triacylglycerol constituents. Significantly higher interaction energy values of the complexes with amino acids suggest a prolonged half-life of the TAG-amino acid systems. The enhanced compatibility between 1,2,3-tripalmitoyl-glycerol (PPP) and amino acids is attributed to the similarity of the dipole moment between these species, resulting in the formation of more stable complexes compared to other combinations. The higher the value of the dipole moment, the more electrically polar the molecule and the more it can polarise the target molecule. These bonds are important to the stabilisation of the transition state of the enzymatic reaction and will have a great impact on overall TAG transformation.

Keywords: DFT, interaction energy, palm oil, transesterification, theoretical approach.

Received: 10 February 2024; **Accepted:** 6 September 2024; **Published online:** 27 November 2024.

INTRODUCTION

Due to recent developments in computational calculations, density functional theory (DFT) approaches have become a main tool for calculations involving various compounds and complexes. Because of its efficiency, the DFT/B3LYP approach has typically been chosen to investigate the molecular geometry and other characteristics of chemical compounds. It provides a great balance between chemical precision and computing expenses. Molecular orbital computation is an aspect of chemistry that is rapidly spreading and has become a useful tool in studying molecular systems prior to their synthesis in the laboratory. It aids in understanding biochemical processes such as enzymatic reactions where it assists with specific properties and leads to the discovery of structure-property-reactivity relationships. As is widely known, the influence of one molecule basis functions augmenting the other molecule causes errors in *ab initio* and DFT calculations of the energetics of intermolecular interactions in complexes. The error arises from the fact that the basic functions of the additional species are typically not included in the calculation of individual molecule energetics. This error known as the basis set superposition

[1] Faculty of Science and Marine Environment, Universiti Malaysia Terengganu, 21030 Kuala Nerus, Terengganu, Malaysia.

* *Corresponding author e-mail: sabiqahanuar@umt.edu.my*

error (BSSE), leads to an incorrect lowering of the complex's total energy. BSSE occurs when the atoms of the interacting molecules or different parts of the same molecule (intermolecular BSSE) approach one another, thus causing their basic functions to overlap.

Over the last 10 years, there has been a growing application of molecular modelling methods to examine the molecular basis of enzyme catalysis. According to recent advancements in the field of computational calculations over the past few years and the availability of more suitable methods, DFT approaches have been employed as one of the primary methods for calculation on various compounds and complexes. Theoretical methods are employed to determine the physical-chemical properties of compounds. The analysis encompasses the examination of molecular geometry, the high-occupied molecular orbital (HOMO)-lowest-unoccupied molecular orbital (LUMO) energy gap, hardness and total energy. The B3LYP computational method has been employed to optimise the structure of $[Cu(H_2PDC)(H_2O)_2]$ (1) complex at various bases sets, including 6-31G (d), 6-31G*, 6-31G** and 6-31++G** (Haghighi et al., 2022). Analysing the energy difference (energy gap) between the HOMO and LUMO is crucial for understanding the characteristics of molecular electrical transport. Numerous computational studies based on quantum mechanics or molecular mechanics approaches have been applied to lipase-catalysed reactions and have helped to elucidate reaction mechanisms or evaluate the role of catalytic amino acids in influencing bioconversion. Increased demand for biodiesel production proves that biodiesel is highly used and has gained the most attention among biofuels as an alternative to conventional fuel (Muhammad et al., 2021). In the context of edible oil transesterification, utilising lipase enzymes as catalysts provides numerous benefits over traditional chemical reactions. Lipase-catalysed biodiesel production holds significant potential for the advancement of an ecologically sustainable and economically viable fuel origin. Triacylglycerols (TAGs) are the main component of vegetable oils. TAGs are molecules made up of one glycerol molecule and three extended hydrocarbon chains connected to it (Long et al., 2021). The composition of the fatty acids, either saturated or unsaturated is important as it affects the fuel properties of biodiesel made from vegetable oil (Khan et al., 2019). In the stoichiometric reaction of transesterification, one mole of TAGs reacts with three moles of alcohol in three consecutive steps, resulting in the formation of fatty acid alkyl esters and glycerol, as shown in *Figure 1*.

A catalyst presence is essential for accelerating the reaction, thereby minimising the formation of intermediate phases, and promoting the efficient formation of the desired product (*Figure 2*).

Based on the literature, it is found that both edible and non-edible oils have been used as feedstocks to produce biodiesels like palm oil, coconut oil, soybean oil, corn oil, sunflower oil, peanut oil, jatropha oil, karanja oil, linseed oil and cottonseed oil, used cooking oil, tallow fat and microalgal (Singh et al., 2019). In countries that produce the most palm oil like Indonesia, Malaysia, Thailand and Colombia it is used as feedstock for biodiesel (Bautista et al., 2019; Kapor et al., 2017; Zahan & Kano, 2018). Palm oil is an attractive feedstock due to its high yield per hectare and low cost to produce biodiesel (Boonrod et al., 2017). The fatty acid profile for vegetable oil can be very complex; for instance, palm oil constituents are mainly palmitic acid (C16:0) and oleic acid (C18:1) (*Table 1*). There are almost equal proportions of saturated and unsaturated fatty acids in palm oil which are palmitic acid (39%-48%), oleic acid (36%-44%) and linoleic acid (9%-12%) (Singh et al., 2020).

In the process of converting vegetable oil into biodiesel, *Candida antarctica* Lipase B (CALB) enzyme was discovered to work well with secondary alcohol to produce branched alkyl esters. This lipase was initially isolated from the yeast *C. antarctica* and is a member of the alpha/beta hydrolase-fold family. CALB catalytic activity is attributed to a serine-histidine-aspartate catalytic triad (Li et al., 2010). Enzymatic catalysis works under ambient pressure and mild conditions. Besides, a fundamental advantage of these enzymes is linked to high substrate specificity, selectivity, regioselectivity and enantioselectivity, where little or no side products are formed, enhancing reaction yields. When compared to other conversion methods, biodiesel and glycerol produced via enzymatic conversion have demonstrated a

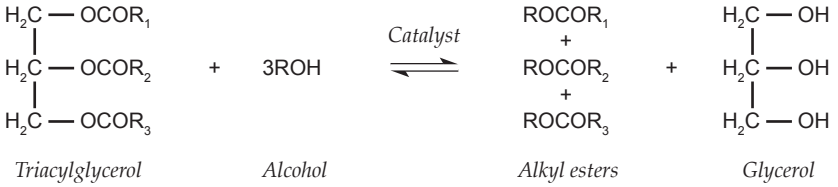

Figure 1. The general chemical reaction depicting the transesterification of TAGs.

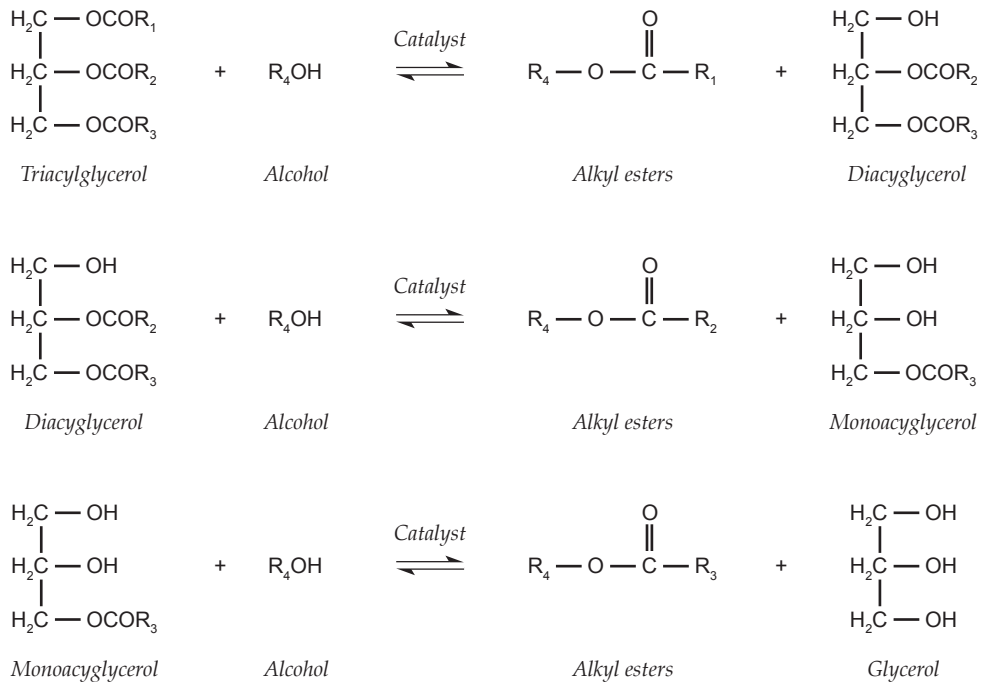

Figure 2. Reversible pathways in the transesterification of vegetable oil form the diacylglycerol and monoacylglycerol intermediates.

TABLE 1. TRIACYLGLYCEROL COMPOSITION (%) OF MALAYSIAN PALM OIL

No double bond (%)		One double bond (%)		Two double bonds (%)		Three double bonds (%)		Four double bonds (%)		Five double bonds (%)	
PPP	6.91	POP	20.02	POO	20.54	PLO	6.59	PLL	1.08	OLL	0.56
		PPO	7.16	PLP	6.36	OOO	5.38	OLO	1.71	LOL	0.14
				OPO	1.86	POL	3.39	OOL	1.76		
				PPL	1.17	OPL	0.61				

Note: P - palmitic acid; O - oleic acid; L - linoleic acid.

greater level of purity. As global energy demands continue to escalate, identifying alternative fuels represents the most effective approach to fulfil this increasing need. It is essential to identify sustainable and environmentally-friendly alternative fuels to support the go green movement and environmental protection. Computes quantum chemistry based on the DFT calculations Gaussian basis set 6-31G** were carried out in these enzyme-substrates complexes indicating three flavonoids (rutin, isoquercitrin and rutin) that are docked in the catalytic cavity of the lipase B from *C. antarctica* (De Oliveira et al. 2010). The CALB enzyme, known for its high enantioselectivity, catalytic activity, substrate versatility and thermal stability, finds widespread use in industrial applications and scientific research. CALB active sites comprise Ser105, His224 and Asp187, with the hydrogen bonds between Ser105 and His224, as well as between Asp187 and His224 playing a crucial role in stabilising the transition state of the enzymatic reaction (Li et al., 2010). Lipases are the most useful sources of the enzymes used in the processes to produce biodiesel (César et al., 2017). Comparing this type of enzyme to others, microbial enzymes can be produced easily and at a low cost due to their abundance, seasonal insensitivity and ease of development, expansion and immobilisation on inexpensive media. Furthermore, compared to other enzymes, microbial-based lipases are more stable and safe for the environment (eco-friendly) (Ureta et al., 2021).

Nevertheless, there is still limited understanding and exploration of the kinetic and physical behaviour of the enzyme-substrate environment. Previous studies have focused on experimental investigations without establishing a correlation between the physical parameters of TAG constituents and the enzymatic transesterification rate of palm olein. To address this gap, this study employs a quantum mechanical approach utilising Gaussian09 software with a DFT level of *ab initio*

molecular simulation to predict the reaction mechanism between the enzyme (specifically lipase) and the substrate in the transesterification process, for biodiesel production. The advancement of computational calculations, particularly DFT methods, has made them highly suitable for predicting the behaviour of different compounds and complexes.

MATERIALS AND METHODS

The Gaussian09 software package programme was employed to do DFT calculations utilising hybrid B3LYP (Frisch et al., 2016). Quantum mechanical calculations were employed using DFT at B3LYP/6-31 G (d,p) level of theory. DFT/ B3LYP produces more precise values although it is similar in computational cost to Hatree-Fock. According to Zabarnick and Phelps (2006), considering the relatively large reaction systems, the DFT technique produced the best results between computational cost and accuracy. The basis set 6-31G (d,p) was used because it was a reasonable compromise between speed and accuracy. For this study, structure drawings were done with GaussView 5.0 (Dennington et al., 2009). The optimisation was done to study the interaction between amino acids and TAG of palm olein. The DFT approach was used to minimise gradients and provide optimised geometries without any symmetry constraints. Eighteen representative TAG fatty acid constituents consisting of palmitoyl, oleoyl and linoleoyl had been selected representing triacylglycerol in palm oil and were used as the neutral molecule, while five amino acids [aspartic acid (Asp), histidine (His), isoleucine (Iso), methionine (Met) and serine (Ser)] represent the enzyme's active sites in *C. antartica* were considered (Kamal et al., 2015). In the cluster approach, the characteristics and reaction mechanism of the enzyme are studied by including a small portion of the enzyme in the model.

RESULTS AND DISCUSSION

The molecules of TAG constituents were first optimised to minimum potential energy and then were forced to form complexes with amino acids (active sites). Quantum chemical models of enzyme active sites have been shown to be highly effective for studying different active site properties as well as reaction mechanisms. The active site is the part of the enzyme which the substrate binds to. Active sites can be extremely sensitive to changes in the enzyme's environment because they are finely tuned to facilitate a chemical reaction. Interaction between H_β TAG substituents and amino acids (active sites) was studied theoretically using Gaussian09. Self-consistent field (SCF) is an initial set of orbitals used to generate a new set of orbitals and the process continues until a set of convergence requirements is met. SCF energy and interaction energy readings between H_β TAG substituents and amino acids (active sites) were collected, listed and ranked according to their efficiency in *Table 2*.

TABLE 2. INTERACTION ENERGY AND DIPOLE MOMENT COMPLEXES OF THE TAG CONSTITUENTS AND AMINO ACIDS

No.	System	E_{int}(uncorr), kJ/mol	E_{int}(corr), kJ/mol	Dipole moment complexes of amino acids with TAG constituents (Debye, D)
1.	PPP + amino acid	-343.925	-307.505	2.7083
2.	OOP + amino acid	-330.437	-293.226	3.6326
3.	POP + amino acid	-326.957	-288.855	2.9827
4.	OPO + amino acid	-292.166	-255.710	2.8498
5.	OLO + amino acid	-292.487	-254.819	3.4720
6.	OPP + amino acid	-292.479	-254.322	2.9560
7.	LPL + amino acid	-292.092	-253.794	3.0931
8.	LPO + amino acid	-290.302	-252.054	2.8766
9.	LPP + amino acid	-289.935	-252.046	3.0081
10.	LLO + amino acid	-288.812	-250.966	3.5016
11.	OLP + amino acid	-287.405	-250.957	3.7051
12.	LOL + amino acid	-288.694	-250.607	3.0487
13.	LLL + amino acid	-288.895	-250.294	3.1448
14.	OOO + amino acid	-288.804	-250.253	3.0456
15.	LLP + amino acid	-287.399	-250.050	3.7485
16.	PLP + amino acid	-287.677	-249.006	3.3503
17.	LOO + amino acid	-286.360	-247.509	2.9831
18.	LOP + amino acid	-284.211	-246.079	3.7310

Note: P - palmitic acid; O - oleic acid; L - linoleic acid.

Results from the calculation showed that the interaction energy for complexes of TAG tripalmitin or 1,2,3-tripalmitoyl-glycerol (PPP) are higher compared to TAG triolein or 1,2,3-trioleoyl-glycerol (OOO) and TAG trilinolein or 1,2,3-trilinoleoyl-glycerol (LLL). The performance of more saturated, TAG PPP has good compatibility with higher interaction energy of -343.925 kJ/mol compared to other TAG (E_{int} LLL + amino acid = -288.895 kJ/mol and E_{int} OOO + amino acid = -288.804 kJ/mol). The higher value of interaction energy of the complexes is due to the compatibility of the species in the complexes. As we know, saturated fatty acids are more stable and have better stability than polyunsaturated fatty acids. A high concentration of polyunsaturated fatty acid can enhance the level of unsaturation of the product and can lead to low cetane number values and oxidation stability of biodiesel (Carvalho et al., 2018). Mainly, palm oil is characterised by a higher content of palmitic acid ester (41.8-46.8 wt%), oleic acid ester (37.3-40.8 wt%) and in minor proportion of linoleic acid ester (9.1-11.0 wt%) (Jiménez-Cruz et al., 2021). In this study, the interaction between TAG and amino acids was examined through two distinct methods: Simple energy calculations and counterpoise corrected energy calculations (BSSE). The BSSE-corrected energy calculations are particularly valuable as they account for errors arising from the superposition of finite basis sets when the species interact. BSSE is related to the incomplete and unbalanced quantum chemical description of the molecules in clusters or complexes. The common method to eliminate the BSSE is the counterpoise (CP) method whereby the BSSE is established using means of mixed basis sets and by performing all the computations again and again, then the error is subtracted recursively from the uncorrected energy. The value of interaction energy was obtained through the computation of interaction energy, and the following formula is shown in Equation (1).

$$\Delta E\ Interaction_{(corrected)} = \Delta E\ Interaction_{(uncorrected)} + \Delta E\ BSSE \qquad (1)$$

After correcting for BSSE, the interaction energies exhibit a revised range of -246.079 to -307.505 kJ/mol. The higher value of interaction energy of the complexes is due to the compatibility of the species in the complexes. Saturated fatty acids are generally more stable and have better stability than polyunsaturated fatty acids. The DFT-optimised geometries of the complexes are shown in *Figure 3*.

Analysis of the calculated interaction energies reveals that the complex between 1,2,3-tripalmitoyl-glycerol (TAG PPP) and amino acids exhibits the highest interaction energy among all the 18 types

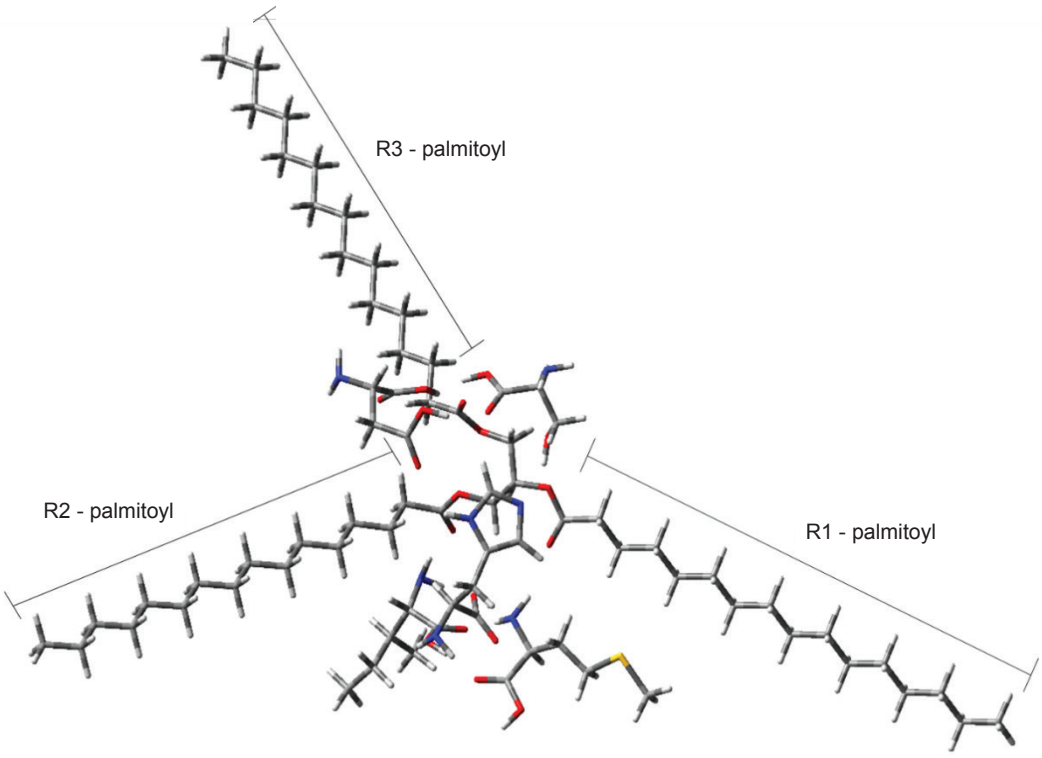

Figure 3. DFT-optimised geometries of the complex 1,2,3-tripalmitoyl-glycerol (TAG PPP) and amino acids (active sites) ($E_{int\ (corr)}$ = -307.505 kJ/mol).

of TAGs, with a value of -307.505 kJ/mol. This is followed by the complexes of 1,2-dioleoyl-3-palmitoyl-glycerol (TAG OOP) and amino acids (-293.226 kJ/mol) and 1,3-dipalmitoyl-2-oleoyl-glycerol (TAG POP) and amino acids (-288.855 kJ/mol). The interaction energies of the remaining complexes are approximately around -250 kJ/mol. The complexes formed between TAG PPP, TAG OOP and TAG POP with amino acids exhibited remarkable compatibility and increase stability compared to the other complexes studied. This enhanced compatibility is expected to result in synergistic effects between the substrate (PPP) and the enzyme (amino acid). Palmitic and oleic acids are the main fatty acids in palm oil. The observed high compatibility between PPP and amino acids can be attributed to the similarities in dipole moments between the species within the complex. Specifically, the dipole moments of PPP (μPPP = 2.7083 D) and the amino acids (μIso = 1.4702 D; μAsp = 1.9976 D; μSer = 2.4280 D; μMet = 3.0373 D; μHis = 8.3957 D) align closely, facilitating stronger interactions and a more stable complex formation. As a result, the PPP molecule forms a more stable complex with amino acids compared to the other complexes studied.

A higher dipole moment value suggests that the molecule has higher electrical polarity and can polarise the target molecule considerably. This prediction will contribute to the interaction of the complexes of TAG constituents and amino acids. These findings align with previous study which has demonstrated how the reaction rates of protease-catalysed transesterification reactions increase with decreasing chain length of the acyl donor and increasing size of the acyl acceptor. Specifically, previous research has indicated that *C. antarctica* lipase exhibits higher activity towards short and medium chain fatty acids, while its activity decreases for long chain fatty acids (Pedersen et al., 2002). The findings reveal that the complex formed between TAG POL and amino acids displays the lowest interaction energy (-246.079 kJ/mol), corresponding to its lowest dipole moment of 3.7310 D (*Figure 4*). The hydrolysis of triacylglycerols by lipases involves a two-step catalytic mechanism: Acylation and deacylation. These reactions are facilitated by the presence of a catalytic triad consisting of three crucial amino acid residues: Ser, His and Asp.

The quantum chemical properties of molecules enable us to determine their energy states utilised in molecular electronics. Kinetic energy is the result of molecules moving in space which is derived from chemical bonds. In addition to the chemical reaction, which is the rearranging of atoms, other chemical energy sources include the vibrations and rotations of molecules. The chemical reactivities of TAG molecules

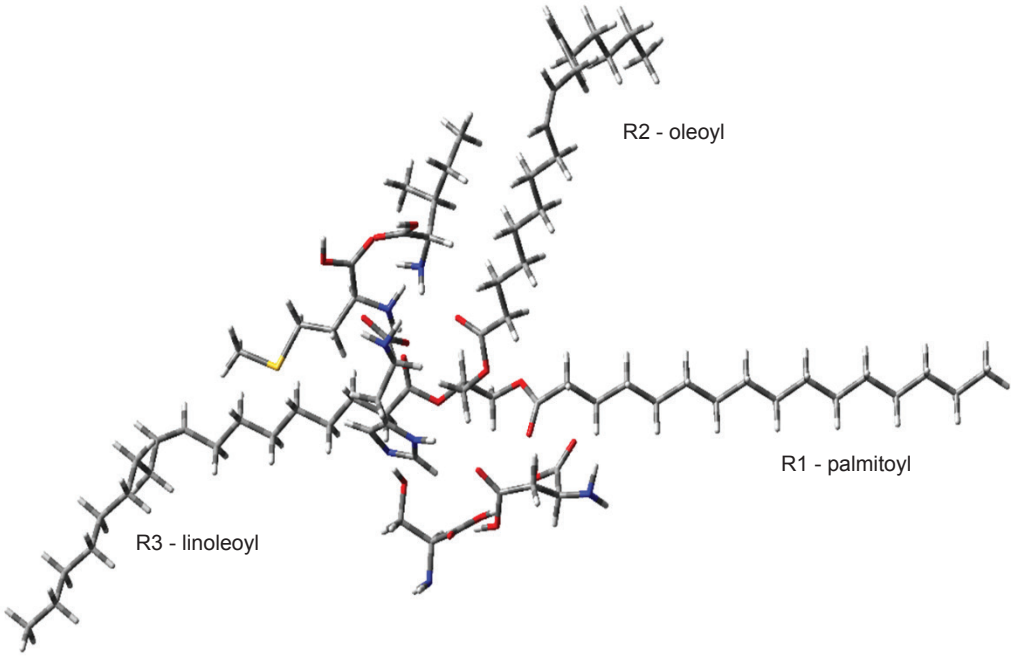

Figure 4. DFT-optimised geometries of the complex 1-palmitoyl-2-oleoyl-2-linoleoyl-rac-glycerol (TAG POL) and amino acids (active sites) ($E_{int(corr)}$ = -246.079 kJ/mol).

and complexes were accessed through various electron density-based molecular properties. These properties include E_{HOMO}, E_{LUMO}, chemical hardness, chemical softness, and global electronegativity as tabulated in *Table 3*. HOMO and LUMO energies are quantum mechanical descriptors crucial in understanding a wide range of chemical reactions which indicate the molecules' electron affinity and ionisation potential, respectively. These energies serve as indicators of the molecule's reactivity and can predict the regions of atomic electrophiles and nucleophiles (Rebaz et al., 2020). The HOMO value provides insight into the molecule's ability to donate electrons. In this study, the HOMO-LUMO frontier orbital compositions for TAG constituents and complexes of TAG constituents with amino acids were calculated using the DFT B3LYP 6-31G (d,p) model chemistry.

Table 3 also shows that the HOMO values of TAG constituents are highly similar, with an average value of approximately -0.23 a.u., except for PPP, which exhibits a slightly lower value of -0.26468 a.u. Higher HOMO values indicate a greater tendency of electron transfer to acceptor molecules (Sayin & Karakas, 2013). The LUMO values of the TAG constituents were examined, and it was observed that OOP and PPO exhibited the lowest value of 0.00090 atomic units compared to the other constituents. It is known that only the TAG constituent palmitoyl (PPP) and TAG constituents containing both palmitoyl and oleoyl groups display LUMO values around 0.001 a.u., while TAG constituents consisting of linoleoyl exhibits LUMO values exceeding 0.007 a.u. This finding aligns with the research by Keypour et al. (2015), which suggests that a lower value for the LUMO orbital energy indicates a higher propensity to accept electronic density. Furthermore, it is well-established that the binding ability of an inhibitor to its target molecule increases with an increase in the HOMO energy and a decrease in the LUMO energy of the complex. An additional important parameter to consider is the energy band gap between the HOMO and LUMO orbitals of the complexes. The energy band gap serves as an indicator of the chemical stability of a molecule, as it represents the difference in energy between these frontier orbitals. In this study, the energy band gaps were calculated for both the TAG constituents alone and the complexes formed with amino acids, using the difference in HOMO and LUMO energies obtained from the completed optimisation process. Generally, the energy band gaps of the TAG constituents alone exhibit higher values compared to the complexes formed with amino acids. Specifically, the energy band gap of PPP is computed as 0.26578 atomic units, while OOP and PPO share the same value of 0.23336 atomic units. This indicates that PPP has a higher energy band gap compared to OOP and PPO, which possess the lowest energy band gap values. Prior research by Rebaz et al. (2020) has indicated that a lower energy band gap corresponds to easier electron donation and greater reactivity. Upon combination with amino acids, the energy band gaps of the complexes differ from those of the TAG constituents alone. Notably, the complex of PPO with amino acids exhibits the highest energy band gap with a value of 0.19710 atomic units, while the complex of LLO and amino acids displays the lowest energy band gap with a value of 0.19521 atomic units.

In addition to the energy band gap (E_{gap}), the HOMO and LUMO values offer valuable insights into other important parameters such as chemical hardness (η), softness (σ) and electronegativity (χ). The chemical hardness for a large HOMO-LUMO gap means a hard molecule which is related to the stability of the molecule. A molecule with a large HOMO-LUMO gap indicates that it is less reactive, while a small HOMO-LUMO gap refers to a soft molecule, which is more reactive. PPP exhibits a hardness value of 0.13, slightly higher than other molecules. Chemical hardness, the measure of conversion efficiency, apparently looks like other complexes with a value of 0.12. Intriguingly, upon complex formations between TAG and amino acids, the hardness values of the molecules decrease from 0.12-0.09, while the softness values increase from approximately 8.30-10.20. Among the molecules, PPP exhibits the lowest softness value of 7.53. This implies that soft molecules, characterised by smaller HOMO-LUMO gaps, possess enhanced reactivity compared to hard molecules, particularly when electron transfer or rearrangement is necessary for the reaction. Soft molecules are highly polarisable, with strong chemical reactivities and low kinetic stabilities (Madkour & Elshamy, 2016). Similarly, global electronegativity accounts for the electronic interactions of molecules with their biological targets. The ability of an atom or a functional group to draw electrons or electron density towards itself is known as global electronegativity. Global electronegativity serves as an important parameter for quantifying the affinity of a species to attract electrons, providing valuable insights into the chemical behaviour of molecules [Equation (2)]. The highest global electronegativity value is obtained for complexes of OLO and amino acids (0.11597), whereas it is observed to be the lowest for complexes of PPP and amino acids (0.11447) as listed in *Table 3*.

$$\text{Global electronegativity, } \chi = \frac{-(E_{HOMO}+E_{LUMO})}{2} \qquad (2)$$

TABLE 3. HOMO, LUMO OF TAG CONSTITUENTS AND COMPLEXES OF AMINO ACIDS WITH TAG CONSTITUENTS AND OTHER PARAMETERS CALCULATED BY HOMO AND LUMO

No.	Symbol	HOMO (a.m.u)	LUMO (a.m.u)	Energy band gap (a.u) (E_{gap})	Hardness (η)	Softness (σ)	Global electronegativity (χ)
1.	PPP	-0.26468	0.00110	0.26578	0.13289	7.52502	0.13179
	PPP + amino acid	-0.21293	-0.01601	0.19692	0.09846	10.15641	0.11447
2.	OPO	-0.23428	0.00793	0.24221	0.12111	8.25730	0.11318
	OPO + amino acid	-0.21400	-0.01727	0.19673	0.09837	10.16622	0.11564
3.	OOO	-0.23422	0.00795	0.24217	0.12109	8.25866	0.11314
	OOO + amino acid	-0.21382	-0.01747	0.19635	0.09818	10.18589	0.11565
4.	POL	-0.23420	0.00693	0.24113	0.12057	8.29428	0.11364
	POL + amino acid	-0.21325	-0.01663	0.19662	0.09831	10.17191	0.11494
5.	LLP	-0.23391	0.00719	0.24110	0.12055	8.29531	0.11336
	LLP + amino acid	-0.21392	-0.01690	0.19702	0.09851	10.15125	0.11541
6.	PLO	-0.23391	0.00745	0.24136	0.12068	8.28638	0.11323
	PLO + amino acid	-0.21394	-0.01695	0.19699	0.09849	10.15280	0.11545
7.	PPL	-0.23388	0.00809	0.24197	0.12098	8.26549	0.11289
	PPL + amino acid	-0.21368	-0.01688	0.19680	0.09840	10.16260	0.11528
8.	OLO	-0.23379	0.00762	0.24141	0.12071	8.28466	0.11308
	OLO + amino acid	-0.21418	-0.01776	0.19642	0.09821	10.18226	0.11597
9.	LLL	-0.23338	0.00680	0.24018	0.12009	8.32709	0.11329
	LLL + amino acid	-0.21275	-0.01726	0.19549	0.09775	10.23070	0.11501
10.	LOL	-0.23334	0.00701	0.24035	0.12018	8.32119	0.11317
	LOL + amino acid	-0.21383	-0.01740	0.19643	0.09822	10.18174	0.11562
11.	LPL	-0.23322	0.00732	0.24054	0.12027	8.31463	0.11295
	LPL + amino acid	-0.21372	-0.01733	0.19639	0.09819	10.18382	0.11553
12.	LPO	-0.23307	0.00742	0.24049	0.12025	8.31635	0.11283
	LPO + amino acid	-0.21392	-0.01727	0.19665	0.09833	10.17035	0.11560
13.	PLP	-0.23296	0.00765	0.24061	0.12031	8.31221	0.11266
	PLP + amino acid	-0.21405	-0.01711	0.19694	0.09847	10.15538	0.11558
14.	LLO	-0.23293	0.00706	0.23999	0.11999	8.33368	0.11294
	LLO + amino acid	-0.21273	-0.01752	0.19521	0.09761	10.24538	0.11513
15.	OOL	-0.23288	0.00787	0.24075	0.12038	8.30737	0.11251
	OOL + amino acid	-0.21360	-0.01717	0.19643	0.09822	10.18174	0.11539
16.	POP	-0.23263	0.00108	0.23371	0.11686	8.55761	0.11578
	POP + amino acid	-0.21360	-0.01697	0.19663	0.09832	10.17139	0.11529
17.	OOP	-0.23246	0.00090	0.23336	0.11668	8.57045	0.11578
	OOP + amino acid	-0.21324	-0.01640	0.19684	0.09842	10.16054	0.11482
18.	PPO	-0.23246	0.00090	0.23336	0.11668	8.57045	0.11578
	PPO + amino acid	-0.21387	-0.01677	0.19710	0.09855	10.14713	0.11532

Note: P - palmitic acid; O - oleic acid; L - linoleic acid.

CONCLUSION

In conclusion, several molecular properties can be utilised after the optimisation such as SCF energy, molecular geometry, dipole moment, HOMO and LUMO, energy band gap, hardness, softness, global electronegativity and interaction energy (complexes). Due to the BSSE, the interaction energies exhibit a revised range of -246.079 to -307.505 kJ/mol. Interaction energies reveal that the complex between TAG PPP and amino acids exhibits the highest interaction energy among all the eighteen types of TAGs, while other TAGs have remaining complexes that are approximately around -250.000 kJ/mol. A variety of variables affect biodiesel characteristics, such as the number and position of the double bonds, the degree of unsaturation, molecular weight, and hydroxyl branch groups. Complex PPP molecules form a more stable complex with amino acids than the other complexes studied. The performance of more saturated fatty acid constituents such as TAG PPP is very effective compared to other TAG constituents. These findings align with previous research that has demonstrated how the reaction rates of protease-catalysed transesterification reactions increase with decreasing chain length of the acyl donor and increasing size of the acyl acceptor. The changes in the dipole moment are associated with the hydrogen bonding between

the TAG constituents and amino acids, which is the hydrogen bond between Ser and His and the hydrogen bond between Asp and His.

Much work is still required to understand the kinetics and reaction mechanisms for improving catalyst activity. Since transesterification is well-known as the most efficient biodiesel processing methodology, new catalytic transesterification technology that can consolidate transesterification processes is essential to reduce the gap between the cost of production and biodiesel price. Furthermore, extensive collaboration should be considered to explore the synergistic relationship towards the advancement of biodiesel production in terms of designing and developing of effective catalyst that is suitable at low temperatures, with improved regeneration and high stability. Therefore, we reasoned that to understand the transesterification pathways and intricate transesterification mechanism of the oil with enzymes, comprehensive theoretical calculations of the transesterification would be necessary.

ACKNOWLEDGEMENT

The authors would like to acknowledge the financial support from Universiti Malaysia Terengganu under the Talent and Publication Enhancement – Research Grant Fasa 1/2018 (TAPE-RG-55175) throughout the research. The authors are also thankful to the Research Management Office and the Faculty of Science and Marine Environment, UMT for the technical support and facilities during the conduct of the study.

REFERENCES

Bautista, S., Espinoza, A., Narvaez, P., Camargo, M., & Morel, L. (2019). A system dynamics approach for sustainability assessment of biodiesel production in Colombia – Baseline simulation. *Journal of Cleaner Production*, *213*, 1–20. https://doi.org/10.1016/j.jclepro.2018.12.111

Boonrod, B., Prapainainar, C., Narataruksa, P., Kantama, A., Saibautrong, W., Sudsakorn, K., Mungcharoen, T., & Prapainainar, P. (2017). Evaluating the environmental impacts of bio-hydrogenated diesel production from palm oil and fatty acid methyl ester through life cycle assessment. *Journal of Cleaner Production*, *142*, 1210–1221. https://doi.org/10.1016/j.jclepro.2016.07.128

Carvalho, A. K. F., Bento, H. B. S., Rivaldi, J. D., & De Castro, H. F. (2018). Direct transesterification of *Mucor circinelloides* biomass for biodiesel production: Effect of carbon sources on the accumulation of fungal lipids and biodiesel properties. *Fuel*, *234*, 789–796. https://doi.org/10.1016/j.fuel.2018.07.029

César, A. D. S., Werderits, D. E., Saraiva, G. L. D. O., & Guabiroba, R. C. D. S. (2017). The potential of waste cooking oil as supply for the Brazilian biodiesel chain. *Renewable and Sustainable Energy Reviews*, *72*, 246–253. https://doi.org/10.1016/j.rser.2016.11.240

De Oliveira, E. B., Humeau, C., Maia, E. R., Chebil, L., Ronat, E., Monard, G., Ruiz-Lopez, M. F., Ghoul, M., & Engasser, J. M. (2010). An approach based on density functional theory (DFT) calculations to assess the *Candida antarctica* lipase B selectivity in rutin, isoquercitrin and quercetin acetylation. *Journal of Molecular Catalysis B: Enzymatic*, *66*, 325–331. https://doi.org/10.1016/j.molcatb.2010.06.009

Dennington, R., Keith, T., & Millam, J. (2009). *GaussView (Version 5)*. Semichem Inc.

Frisch, M. J., Trucks, G. W., Schlegel, H. B., Scuseria, G. E., Robb, M. A., Cheeseman, J. R., Scalmani, G., Barone, V., Petersson, G. A., Nakatsuji, G. E., Li, X., Caricato, M., Marenich, A., Bloino, J., Janesko, B. G., Gomperts, R., Mennucci, B., & Hratchi, S. (2016). *Gaussian09 (Revision A.02)*. Gaussian, Inc.

Haghighi, M., Zare, L. B., & Ghiasi, M. (2022). Biodiesel production from spirulina algae oil over [Cu(H_2PDC) (H_2O)$_2$] complex using transesterification reaction: Experimental study and DFT approach. *Chemical Engineering Journal*, *430*, 132777. https://doi.org/10.1016/j.cej.2021.132777

Jiménez-Cruz, F., Marín-Rosas, C., Castañeda-Lopez, L. C., & García-Gutiérrez, J. L. (2021). Promising extruded catalyst for palm oil transesterification from $LiAlH_4$ hydrolysates. *Arabian Journal of Chemistry*, *14*(10), 103141. https://doi.org/10.1016/j.arabjc.2021.103141

Kamal, M. Z., Barrow, C. J., & Rao, N. M. (2015). A computational search for lipases that can preferentially hydrolyze long-chain omega-3 fatty acids from fish oil triacylglycerols. *Food Chemistry*, *173*, 1030–1036. https://doi.org/10.1016/j.foodchem.2014.10.124

Kapor, N. Z. A., Maniam, G. P., Rahim, M. H. A., & Yusoff, M. M. (2017). Palm fatty acid distillate as a potential source for biodiesel production – A review. *Journal of Cleaner Production*, *143*, 1–9. https://doi.org/10.1016/j.jclepro.2016.12.163

Keypour, H., Rezaeivala, M., Mirzaei-Monsef, M., Sayin, K., Dilek, N., & Unver, H. (2015). Synthesis and characterization of Co(II), Ni(II), Cu(II) and Zn(II) complexes with a new homopiperazine macrocyclic Schiff base ligand. *Inorganica Chimica Acta*, *432*, 243–249. https://doi.org/10.1016/j.ica.2015.04.017

Khan, S., Lup, A. N. K., Qureshi, K. M., Abnisa, F., Daud, W. M. A. W., & Patah, M. F. A. (2019). A review on deoxygenation of triglycerides for jet fuel range hydrocarbons. *Journal of Analytical and Applied Pyrolysis*, *140*, 1–24. https://doi.org/10.1016/j.jaap.2019.03.005

Li, C., Tan, T., Zhang, H., & Feng, W. (2010). Analysis of the conformational stability and activity of *Candida antarctica* lipase B in organic solvents. Insight from molecular dynamics and quantum mechanics/simulations. *Journal of Biological Chemistry*, *285*(38), 28434–28441. https://doi.org/10.1074/jbc.M110.136200

Long, F., Liu, W., Jiang, X., Zhai, Q., Cao, X., Jiang, J., & Xu, J. (2021). State-of-the-art technologies for biofuel production from triglycerides: A review. *Renewable and Sustainable Energy Reviews*, *148*, 111269. https://doi.org/10.1016/j.rser.2021.111269

Madkour, L. H., & Elshamy, I. H. (2016). Experimental and computational studies on the inhibition performances of benzimidazole and its derivatives for the corrosion of copper in nitric acid. *International Journal of Industrial Chemistry*, *7*(3), 195–221. https://doi.org/10.1007/s40090-015-0070-8

Muhammad, G., Alam, M. A., Mofijur, M., Jahirul, M. I., Lv, Y., Xiong, W., Ong, H. C., & Xu, J. (2021). Modern developmental aspects in the field of economical harvesting and biodiesel production from microalgae biomass. *Renewable and Sustainable Energy Reviews*, *135*, 110209. https://doi.org/10.1016/j.rser.2020.110209

Pedersen, N. R., Wimmer, R., Emmersen, J., Degn, P., & Pedersen, L. H. (2002). Effect of fatty acid chain length on initial reaction rates and regioselectivity of lipase-catalysed esterification of disaccharides. *Carbohydrate Research*, *337*(13), 1179–1184. https://doi.org/10.1016/S0008-6215(02)00112-X

Rebaz, O., Koparir, P., & Ahmed, L. (2020). Computational determination the reactivity of salbutamol and propranolol drugs. *Turkish Computational and Theoretical Chemistry*, *4*(2), 67–75. https://doi.org/10.33435/tcandtc.768758

Sayin, K., & Karakas, D. (2013). Quantum chemical studies on the some inorganic corrosion inhibitors. *Corrosion Science*, *77*, 37–45. https://doi.org/10.1016/j.corsci.2013.07.023

Singh, D., Sharma, D., Soni, S. L., Sharma, S., & Kumari, D. (2019). Chemical compositions, properties, and standards for different generation biodiesels: A review. *Fuel*, *253*, 60–71. https://doi.org/10.1016/j.fuel.2019.04.174

Singh, D., Sharma, D., Soni, S. L., Sharma, S., Sharma, P. K., & Jhalani, A. (2020). A review on feedstocks, production processes, and yield for different generations of biodiesel. *Fuel*, *262*, 116553. https://doi.org/10.1016/j.fuel.2019.116553

Ureta, M. M., Martins, G. N., Figueira, O., Pires, P. F., Castilho, P. C., & Gomez-Zavaglia, A. (2021). Recent advances in β-galactosidase and fructosyltransferase immobilization technology. *Critical Reviews in Food Science and Nutrition*, *61*(16), 2659–2690. https://doi.org/10.1080/10408398.2020.1783639

Zabarnick, S., & Phelps, D. K. (2006). Density functional theory calculations of the energetics and kinetics of jet fuel autoxidation reactions. *Energy & Fuels*, *20*(2), 488–497. https://doi.org/10.1021/ef0503481

Zahan, K. A., & Kano, M. (2018). Biodiesel production from palm oil, its by-products, and mill effluent: A review. *Energies*, *11*(8), 2132. https://doi.org/10.3390/en11082132